

# SI-CLP inhibits the growth of mouse mammary adenocarcinoma by preventing recruitment of tumor-associated macrophages

Shuiping Yin<sup>1,2</sup>, Nan Wang<sup>3,4</sup>, Vladimir Riabov<sup>1,5</sup>, Dieuwertje M. Mossel<sup>1</sup>, Irina Larionova<sup>5,6</sup>, Kai Schledzewski<sup>3</sup>, Olga Trofimova<sup>7</sup>, Tatyana Sevastyanova<sup>1</sup>, Anna Zajakina<sup>7</sup>, Christina Schmuttermaier<sup>1</sup>, Alexei Gratchev<sup>3,8</sup>, Andrew Flatley<sup>9</sup>, Elisabeth Kremmer<sup>9</sup>, Marina Zavyalova<sup>6</sup>, Nadezhda Cherdyntseva<sup>5,6</sup>, Katja Simon-Keller<sup>10</sup>, Alexander Marx<sup>10</sup>, Harald Klüter<sup>1,11</sup>, Sergij Goerdts<sup>3</sup> and Julia Kzhyshkowska<sup>1,5,11</sup>

<sup>1</sup>Medical Faculty Mannheim, Institute for Transfusion Medicine and Immunology, Ruprecht-Karls University of Heidelberg, Mannheim, Germany

<sup>2</sup>Department of Urology, The First Affiliated Hospital of Anhui Medical University, Hefei, Anhui, China

<sup>3</sup>Department of Dermatology, Medical Faculty Mannheim, Ruprecht-Karls University of Heidelberg, Mannheim, Germany

<sup>4</sup>Department of Otolaryngology-Head and Neck Surgery, Tongji Hospital, Tongji Medical College, Huazhong University of Science and Technology, Wuhan, China

<sup>5</sup>Laboratory of Translational Cellular and Molecular Biomedicine, Tomsk State University, Tomsk, Russia

<sup>6</sup>Cancer Research Institute, Tomsk National Research Medical Center of the Russian Academy of Sciences, Tomsk, Russia

<sup>7</sup>Latvian Biomedical Research and Study Centre, Riga, Latvia

<sup>8</sup>Laboratory for Tumor Stromal Cell Biology, Institute of Carcinogenesis, NN Blokhin Cancer Research Center, Russian Academy of Sciences, Moscow, Russia

<sup>9</sup>Institute of Molecular Immunology, Helmholtz Zentrum München, German Research Center for Environmental Health (GmbH), Munich, Germany

<sup>10</sup>Institute of Pathology, Medical Faculty Mannheim, Ruprecht-Karls University of Heidelberg, Mannheim, Germany

<sup>11</sup>German Red Cross Blood Service Baden-Württemberg – Hessen, Mannheim, Germany

Chitinase-like proteins (CLP) are chitin-binding proteins that lack chitin hydrolyzing activity, but possess cytokine-like and growth factor-like properties, and play crucial role in intercellular crosstalk. Both human and mice express two members of CLP family: YKL-40 and stabilin-1 interacting chitinase-like protein (SI-CLP). Despite numerous reports indicating the role of YKL-40 in the support of angiogenesis, tumor cell proliferation, invasion and metastasis, the role of its structurally related protein SI-CLP in cancer was not reported. Using gain-of-function approach, we demonstrate in the current study that the expression of recombinant SI-CLP in mouse TS/A mammary adenocarcinoma cells results in significant and persistent inhibition of *in vivo* tumor growth. Using quantitative immunohistochemistry, we show that on the cellular level this phenomenon is associated with reduced infiltration of tumor-associated macrophages (TAMs), CD4+ and FoxP3+ cells in SI-CLP expressing tumors. Gene expression analysis in TAM isolated from SI-CLP-expressing and control tumors demonstrated that SI-CLP does not affect macrophage phenotype. However, SI-CLP significantly inhibited migration of murine bone-marrow derived macrophages and human primary monocytes toward monocyte-recruiting chemokine CCL2 produced in the tumor microenvironment (TME). Mechanistically, SI-CLP did not affect CCL2/CCR2 interaction, but suppressed cytoskeletal rearrangements in response to CCL2. Altogether, our data indicate that SI-CLP functions as a tumor growth inhibitor in mouse breast cancer by altering cellular composition of TME and blocking cytokine-induced

**Additional Supporting Information** may be found in the online version of this article.

**Key words:** chitinase-like proteins, SI-CLP, tumor-associated macrophages, breast cancer, CCL2, tumor microenvironment

**Abbreviations:** BMDM: bone-marrow derived macrophages; CLP: chitinase-like proteins; EV: empty vector; SFV: Semliki Forest Virus;

SI-CLP: stabilin-1 interacting chitinase-like protein; TME: tumor microenvironment; TAM: tumor-associated macrophages; WT: wild-type

**Conflict of interest:** The authors declare that there is no conflict of interest regarding the publication of this article.

Shuiping Yin, Nan Wang and Vladimir Riabov equally contributed to this work

**Grant sponsor:** China Scholarships Council; **Grant numbers:** 2009616122, 201208080046; **Grant sponsor:** ERA.NET RUS DTEST-CLP;

**Grant sponsor:** ERA.Net RUS Plus CHIT-ALPHA-THER; **Grant sponsor:** Russian Science Foundation; **Grant number:** 14-15-00350

This is an open access article under the terms of the Creative Commons Attribution-NonCommercial-NoDerivs License, which permits use and distribution in any medium, provided the original work is properly cited, the use is non-commercial and no modifications or adaptations are made.

**DOI:** 10.1002/ijc.32685

**History:** Received 13 Sep 2018; Accepted 7 Aug 2019; Online 16 Sep 2019

**Correspondence to:** Prof. Dr. Julia Kzhyshkowska, Institute of Transfusion Medicine and Immunology, Medical Faculty Mannheim, Heidelberg University, Theodor-Kutzer-Ufer 1-3, 68167, Mannheim, Germany, Tel.: +49-621-383-9723, Fax: +49-621-383-9721, E-mail: julia.kzhyshkowska@medma.uni-heidelberg.de

**TAM recruitment.** Taking into consideration weak to absent expression of SI-CLP in human breast cancer, it can be considered as a therapeutic protein to block TAM-mediated support of breast tumor growth.

#### What's new?

Chitinase-like proteins possess cytokine-like properties and can manipulate cancer progression. Here the authors show that stabilin-1 interacting chitinase-like protein (SI-CLP) inhibits the growth of murine mammary adenocarcinoma by altering the tumor microenvironment and reducing intratumoral macrophage infiltration. SI-CLP is weakly expressed in human breast cancers and may function as a possible therapeutic agent to suppress breast cancer growth.

#### Introduction

Tumor microenvironment (TME) that consists of multiple immune and nonimmune cells, blood vessels, signaling molecules and extracellular matrix is an important factor that influences the growth, migration, invasion and metastatic spread of cancer cells.<sup>1</sup> Among components of TME, immune cells largely contribute to the processes of tumor cell recognition and elimination. However, under persistent influence of molecular signals derived from cancer cells and other components of TME, immune cells are reprogrammed to foster tumor progression by producing immunosuppressive, prosurvival and proangiogenic factors.<sup>2,3</sup> Tumor-associated macrophages (TAMs) are one of the major immune cell types in the TME of solid cancers. In advanced breast cancer, TAMs are the most abundant infiltrating leukocytes in the tumor tissue that produce wide range of soluble mediators including anti-inflammatory/immunosuppressive cytokines (IL-10, TGF- $\beta$ ), angiogenic molecules (e.g., VEGF-A, C, D, MMP-9) and growth factors (e.g., EGF, PDGF) responsible for induction of tumor cell proliferation, vascularization, acquisition of resistance to chemotherapy and deactivation of adaptive immune response.<sup>4</sup> Thus, several TAM-targeting approaches were developed in order to reduce their recruitment and accumulation in the tumor tissue.<sup>5</sup> These approaches utilized blocking antibodies or small molecule inhibitors toward cytokines/cytokine receptor axes such as CSF-1/CSF-1R and CCL2/CCR2 that are critical for macrophage accumulation and survival in the tumors.<sup>5</sup> For example, CCL2 neutralization using monoclonal antibodies carlumab transiently suppressed free serum CCL2 in prostate and breast cancer patients.<sup>6,7</sup> However, complete inhibition of CCR2/CCL2 axis was not achieved.<sup>6</sup> In addition, discontinuation of anti-CCL2 treatment in mouse breast cancer model was associated with mobilization of monocytes from bone marrow, their influx in the tumor and lungs resulting in metastatic relapse.<sup>8</sup> Therefore, exploration of novel molecular factors that may prevent accumulation of TAM in breast and other types of solid cancers is of relevance. Among these factors, chitinase-like proteins (CLP) were reported to influence TAM recruitment.<sup>9</sup>

CLP are chitin-binding proteins that lack chitin-hydrolyzing activity, but possess cytokine-like and growth factor-like

properties.<sup>9</sup> In human, proteins of CLP family are represented by YKL-40, YKL-39 and stabilin-1 interacting chitinase-like protein (SI-CLP). In mice, CLP members include YKL-40, SI-CLP and Ym1/Ym2. CLP are expressed in multiple cell types including chondrocytes, neutrophils, macrophages and tumor cells. In the TME, CLP protein YKL-40 is involved in the regulation of tumor cell proliferation, migration, invasion and angiogenesis.<sup>9</sup> YKL-40 is the most characterized member of CLP family and its plasma and intratumoral levels are associated with poor prognosis in many types of tumors including breast and colon cancers, glioblastoma, melanoma etc.<sup>9</sup> Besides its proinvasive properties for tumor cells, YKL-40 was shown to stimulate the release of macrophage chemoattractants CCL2 and IL-8 from tumor cells resulting in macrophage recruitment *in vivo*.<sup>10</sup> Another member of CLP family YKL-39 was found to induce monocyte migration and angiogenesis *in vitro*; its intratumoral expression levels in breast cancer were predictive for increased risk of metastasis after neoadjuvant chemotherapy.<sup>11</sup> Despite the involvement of YKL-40 and YKL-39 in the tumor progression and monocyte/macrophage recruitment, the role of structurally related CLP protein SI-CLP in the regulation of macrophage migration and tumor growth is unknown. SI-CLP is expressed in human alternatively activated macrophages stimulated by the combination of IL-4 and dexamethasone and its expression was found to be elevated in peripheral blood mononuclear cells of rheumatoid arthritis patients.<sup>12,13</sup> In mice, SI-CLP expression in bone marrow macrophages was stimulated by IL-12 and IL-13.<sup>13</sup> Currently, established function of SI-CLP is restricted to aggravation of inflammatory response in a mouse model of rheumatoid arthritis.<sup>13</sup>

Using mouse model of TS/A mammary adenocarcinoma engineered to express mouse SI-CLP protein, we report an inhibitory effect of SI-CLP on tumor growth which was associated with significant reduction in intratumoral TAM infiltration. However, SI-CLP expression in the tumor did not influence the phenotype of TAM. Using *in vitro* migration assays in human and mouse macrophages, we show that purified SI-CLP protein as well as SI-CLP containing supernatants prevent macrophage migration toward TAM-recruiting chemokine CCL2, indicating that anti-tumor effect of SI-CLP is mediated by blockade of intratumoral macrophage recruitment.

## Materials and Methods

### Human breast cancer specimens

Tumor samples of 28 female patients with breast cancer T1-4N0-3M0-1 seen at the University Medical Center Mannheim, Germany and 52 female patients with nonspecific invasive breast cancer T1-4N0-3M0 seen at General Oncology Department of Tomsk Cancer Research Institute (Tomsk, Russia) were used in the study. All studies were approved by the ethics and review committee of Medical Faculty Mannheim, University of Heidelberg (approval number: 2015-807R-MA) and the Local Committee for Medical Ethics of Tomsk Cancer Research Institute (protocol No. 13 from September 27, 2014), and informed consents were obtained from all patients prior to analysis. Patients did not receive preoperative treatment. The mean age of women with breast cancer in German cohort was  $64.3 \pm 11.8$  years and in Russian cohort was  $61.3 \pm 10.4$  years. The histological type of breast cancer was defined according to the WHO recommendations (Geneva, 2012) and corresponded to nonspecific invasive carcinoma in all cases. Clinical data of patients are presented in Supporting Information Tables S2 and S3.

### Generation of SI-CLP expressing TS/A cells

Full-length murine SI-CLP (mChid1) fused to the N-terminal FLAG-tag was generated using pcDNA3.1 expression vector (Invitrogen, Carlsbad, CA) containing FLAG sequence. TS/A murine mammary adenocarcinoma cell line (RRID:CVCL\_F736) was kindly provided by Dr. Patrizia Nanni (Istituto di Cancerologia, Università di Bologna, Bologna, Italy) and propagated as described previously.<sup>14</sup> TS/A cells were transfected with pcDNA3.1-SI-CLP-FLAG or pcDNA3.1-FLAG (empty vector control) constructs using FuGeneHD transfection reagent (Roche, Basel, Switzerland) and single clones were selected using 700  $\mu\text{g}/\text{ml}$  of G418 (Sigma-Aldrich, St. Louis, MO). SI-CLP expression in TS/A clones was visualized using anti-SI-CLP monoclonal antibodies, clone 1B8 (rat IgG2a/k; generated and validated in collaboration with Dr. Elisabeth Kremmer; Helmholtz Zentrum, Munich) by immunofluorescent microscopy. Five SI-CLP clones and five vector clones were selected for further experiments. All experiments were performed with mycoplasma-free cells.

### Animal tumor model

Balb/c wild-type (WT) female mice of 8–10 weeks old were purchased from Janvier Labs. All mice were housed under specific pathogen-free conditions at the animal facility in Mannheim. All animal experiments were approved by the Medical Ethics Committee II of the Medical Faculty Mannheim of the University of Heidelberg and filed with local authorities (Regierungspräsidium Karlsruhe). Three TS/A-EV tumor clones (TS/A-P320-A1, TS/A-P320-A2 and TS/A-P320-CL1) and three TS/A-SI-CLP tumor clones (TS/A-P776-PID5, TS/A-P776-P2B7 and TS/A-P776-P1F10) were used in the tumor growth experiments. Mice were

injected subcutaneously in the right flank with  $2.5 \times 10^6$  of TS/A-EV or TS/A-SI-CLP cells in PBS. Tumor size was measured by caliper on Days 7, 10, 14, 18 and 21 postinjection, and tumor volume (in  $\text{mm}^3$ ) was calculated using following formula: tumor volume =  $0.52 \times \text{length} \times \text{width} \times \text{thickness}$ . Tumor weight was measured on Day 21 postinjection.

### Immunohistochemistry

Acetone-fixed frozen sections of TS/A tumors (5  $\mu\text{m}$  thickness) were analyzed using following primary antimouse antibodies: rat CD68 (Acris, Herford, Germany), rat CD31, rat CD206 (both from AbD Serotec, Hercules, CA), rabbit stabilin-1 (clone RS1, self-produced), rat Siglec-F, rat CD8a, rat FoxP3-biotin (all from eBioscience, San Diego, CA), rat-anti mouse Ly6G antibodies (Abcam, Cambridge, MA; ab25377) and rat CD4-biotin (BioLegend, San Diego, CA). HRP conjugated goat antirat IgG (Santa Cruz Biotechnology, Dallas, TX), HRP conjugated goat antirabbit IgG (Acris), and HRP conjugated streptavidin (Jackson ImmunoResearch, West Grove, PA) were used as secondary reagents. Sections were developed using AEC Chromogen Substrate (Dako Cytomation, Glostrup, Denmark) and counterstained with Mayer's Haemalaun solution (Merck, Kenilworth, NJ). Entire sections were scanned as described previously<sup>14</sup> and staining intensity (positivity) was analyzed using Aperio ImageScope software (free from Aperio.com).

Paraffin embedded, formalin fixed, human breast cancer tissue sections (1  $\mu\text{m}$  thickness) were incubated in HIER T-EDTA Buffer pH 9.0 (Zytomed, Berlin, Germany) for 15 min in water bath at 80°C and stained using rat antihuman SI-CLP antibodies, clone 1C11,<sup>12</sup> followed by antirat-HRP labeled antibodies (Santa Cruz Biotechnology) or Super Sensitive Polymer-HRP detection system was used (BioGenex, Fremont, CA). Sections were developed using AEC Chromogen Substrate (Dako Cytomation) and counterstained with Mayer's Haemalaun solution (Merck). Images were acquired using Carl Zeiss Axio Lab.A1 light microscope (Jenamed, Carl Zeiss, Germany) and Leica DC500 digital camera. To analyze the association between SI-CLP expression and patients clinical parameters, all patients in Russian cohort were distributed into SI-CLP positive and SI-CLP negative groups upon microscopic assessment of stained sections.

### Immunofluorescence/confocal microscopy

Primary monocytes isolated from healthy donors were incubated with purified recombinant SI-CLP (Cusabio, Wuhan, China) at the concentration 100 ng/ml for 16 hr followed by stimulation with CCL2 for 30 min. Cells were fixed at RT in 2% PFA for 10 min, permeabilized in 0.5% Triton X-100 for 15 min followed by additional fixation in 4% PFA for 10 min and stained using antitubulin antibodies (Sigma, T9026, 1:1000) for 1 hr, RT. Secondary FITC-labeled antimouse antibodies (Sigma, F2883, 1:100) were added to the cells for 2 hr, RT together with rhodamine-phalloidin (100 nM, PHDR1, Cytoskeleton). Images were acquired using Leica SP8 confocal microscope.

### Isolation of mouse bone-marrow derived macrophages and TAM

Bone-marrow derived macrophages (BMDM) derived from Balb/c female WT mice were differentiated from bone marrow precursor cells in DMEM + GlutaMAX medium supplemented with 10% FBS and 30 ng/ml of M-CSF for 4 days. TAMs were isolated from TS/A tumors as described previously.<sup>14</sup> TAM purity was greater than 95% as assessed by immunofluorescence staining using rat antimouse CD68 antibodies (Acris). For gene expression analysis, TAMs were lysed immediately after isolation. For assessment of cytokine production in supernatants, TAMs were cultured for 16 hr in DMEM + GlutaMAX medium supplemented with 10% FBS.

### Isolation of mouse splenic T cells

Spleens of WT Balb/c female mice were mechanically disintegrated to obtain single cell suspension followed by red blood cell lysis and positive selection using CD3 MACS beads (Miltenyi Biotec, Bergisch Gladbach, Germany). Cell purity was assessed using flow cytometry and anti-CD3 antibodies (BioLegend). T cells were maintained in RPMI medium for 4 hr, 37°C, 7.5% CO<sub>2</sub> prior to migration assay.

### Isolation of human CD14+ monocytes

Monocytes were isolated from buffy coats of healthy donors using positive magnetic selection with CD14 MACS beads (Miltenyi Biotec) as described previously.<sup>15</sup>

### Gene expression analysis (RT-qPCR)

RNA was isolated from TAM using RNeasy midi kit (Qiagen, Hilden, Germany). Synthesis of cDNA was performed using Superscript II reverse transcriptase (Invitrogen). The expression of TNF $\alpha$ , IL-1 $\beta$ , IL-6, IL-10, TGF $\beta$ , CD206, stabilin-1, CD163 and VEGFA was measured using Taqman RT-qPCR and normalized to the expression of  $\beta$ -actin. Primer sequences are presented in Supporting Information Table S1. Ready-to-use Taqman master mixes for mouse Arginase 1 (Mm00475988\_m1), mouse CCR2 (Mm00438270\_m1), mouse IL10 (Mm00439614\_m1) and mouse TGF- $\beta$ 1 (Mm01178820\_m1) were purchased from ThermoFisher Scientific (Waltham, MA).

### Production of SI-CLP containing supernatants

SI-CLP-containing and Luc control supernatants were obtained from BHK-21 cell line infected with pSFVEnh/mSI-CLP or pSFVEnh/Luc virus particles. The pSFVEnh/Luc vector was previously described.<sup>16</sup> The new pSFVEnh/mSI-CLP construct was generated by replacing Luc gene in pSFVEnh/Luc vector with full-length mouse SI-CLP gene containing FLAG sequence at C-terminus. The resulting plasmids pSFVEnh/Luc and pSFVEnh/mSI-CLP were used to produce recombinant virus particles in BHK-21 cells as previously described.<sup>17</sup> The cell growth medium containing the infectious recSFV particles was then harvested, filtered through 22  $\mu$ m filters and rapidly frozen in liquid nitrogen, and subsequently

used as a source of recSFV particles for cell infection and SI-CLP containing supernatant production. Infection of BHK-21 cells was done as previously described.<sup>18</sup> Briefly, 5–6  $\times$  10<sup>6</sup> BHK-21 cells were cultured in 75 cm<sup>2</sup> flasks and used for infection with pSFVEnh/Luc and pSFVEnh/mSI-CLP virus particles. For infection, the cells were washed twice with PBS containing Mg<sup>2+</sup> and Ca<sup>2+</sup> (Invitrogen, UK). Next, 5 ml of the virus stock diluted in PBS containing Mg<sup>2+</sup> and Ca<sup>2+</sup> was added at multiplicity of infection (MOI) 5, ensuring the maximal cell infection with 5 IFU per one cell. The cells were incubated for 1 hr in a humidified 5% CO<sub>2</sub> incubator at 37°C. The control cells (uninfected) were incubated with PBS (containing Mg<sup>2+</sup> and Ca<sup>2+</sup>). Cells were washed twice with PBS (Mg<sup>2+</sup> and Ca<sup>2+</sup>) and incubated for 48 hr in 12 ml of cultivation medium supplemented with 1% FBS. After incubation, cell supernatants were harvested, centrifuged at 1,000g for 10 min, filtered through 0.22  $\mu$ m filters, aliquoted and stored frozen at –70°C.

### Immunoprecipitation

For the detection of secreted SI-CLP, cell culture supernatants from TS/A-EV and TS/A-SI-CLP-FLAG stable clones were incubated with Protein G sepharose beads bound to rabbit anti-FLAG antibodies (Sigma) followed by Western blotting using rat anti-SI-CLP antibodies (clone 1B8). For depletion of SI-CLP protein from recSFVEnh/SI-CLP supernatants, rat anti-SI-CLP (1B8) antibodies were immobilized on protein G beads. recSFVEnh/SI-CLP and recSFVEnh/Luc control supernatants (20  $\mu$ l each) were diluted with 800  $\mu$ l DMEM medium and incubated with protein G/1B8 beads for 3 hr, 4°C. Depleted supernatants were collected and analyzed for SI-CLP content using Western blotting and 1B8 antibodies.

### Migration assay

Purified SI-CLP protein derived from HEK293 cells was purchased from Cusabio (Wuhan, China). Before migration assay BMDM, monocytes and T cells were preincubated with recSFVEnh/SI-CLP containing supernatants or purified SI-CLP protein for 30 min or 16 hr as specified in the text. In some of the experiments, SI-CLP was depleted from supernatants using immunoprecipitation with Protein G Sepharose beads conjugated with rat anti-SI-CLP antibody (1B8) followed by control of SI-CLP depletion using Western Blotting and 1B8 antibodies. For migration assay, 6.5 mm Transwell containing polycarbonate membrane inserts (Corning) with 5.0  $\mu$ m pores were used. Culture medium (600  $\mu$ l) containing chemoattractants was added in the lower chamber of transwell. The following chemoattractants were used: 100 ng/ml of purified murine SI-CLP (Cusabio), 100 ng/ml of murine CCL2 for BMDM, 100 ng/ml of human CCL2, 10 ng/ml of CCL5 or 100 ng/ml of CCL7 for monocytes and 100 ng/ml of murine CCL19 for T cells (all from Peprotech). Migration time was 3 hr for all tested immune cells. To count migrated cells on the membrane, nonmigrated

cells were removed from upper side of the membrane using cotton swab. Inserts were fixed in ice-cold methanol (5 min at  $-30^{\circ}\text{C}$ ) and migrated cells on the lower side of membrane were stained using DAPI. Membranes were transferred on microscopic slides and 10 random images were taken using fluorescent microscope equipped with a  $32\times$  objective. Average number of migrated cells was calculated for each condition and chemotactic index was calculated according to the following formula: number of migrated cells in experimental group (SI-CLP)/number of migrated cells in control group.<sup>19</sup>

### CCR2 internalization and recycling assay

Monocytes were cultured for 16 hr in nonsupplemented macrophage SFM medium (Life Technologies, Carlsbad, CA) with or without 100 ng/ml of purified SI-CLP followed by stimulation with 100 ng/ml CCL2 for 5 min,  $37^{\circ}\text{C}$ . In recycling experiments, cells were stimulated with 100 ng/ml CCL2 for 5 min followed by removal of CCL2-containing medium and additional 30 min incubation in chemokine-free SFM medium. Monocytes were replaced on ice for 45 min and detached by scraping. Cells were incubated with Fc-blocking reagent (Miltenyi Biotec) for 5 min at  $+4^{\circ}\text{C}$  and stained using FITC-conjugated anti-CCR2 antibodies (Biolegend, clone K036C2) for 30 min at  $+4^{\circ}\text{C}$ . Cells were washed, incubated with 2.5  $\mu\text{l}$  of 7-AAD (Beckman Coulter, Brea, CA) for 10 min at  $+4^{\circ}\text{C}$  and immediately analyzed using BD FACS Canto II flow cytometer.

### Tumor cell proliferation and migration assays

TS/A-EV and TS/A-SI-CLP cells were maintained in RPMI complete medium until the cell confluence reached approximately 80%. Next, 10  $\mu\text{M}/\text{ml}$  EdU (5-ethynyl-2'-deoxyuridine) was added to the medium and incubated with cells at  $37^{\circ}\text{C}$  for 1 hr. Cell proliferation was measured by flow cytometry using Click-iT<sup>®</sup> EdU Alexa Fluor<sup>®</sup> 488 Flow Cytometry Assay Kit (ThermoFisher Scientific) according to manufacturer instructions. Cell proliferation was analyzed by flow cytometry using BD FACS Canto II flow cytometer. TS/A cell migration from 2% toward 20% FBS was performed for 16 hr using Transwell inserts with 8.0  $\mu\text{m}$  pores (Corning, Corning, NY). The calculation of the number of migrated cells was done as described above.

### Statistical analysis

The data were statistically analyzed using GraphPad Prism 6 software (GraphPad Soft Inc., La Jolla, CA). Unpaired and paired *t* tests as well as Mann–Whitney U test and Wilcoxon signed-ranked test were used to assess the difference between experimental groups as specified in the figure legends. Differences were considered significant at  $p < 0.05$  level. For the analysis of the association between SI-CLP expression with clinical parameters, statistical analysis was performed using STATISTICA 8.0 for Windows (StatSoft Inc., Tulsa, OK). The ANOVA, Fisher's exact test, Chi-square

test and Nonparametrics Mann–Whitney U test were implemented. Statistical significance was set at  $p$  value  $< 0.05$ , with a two-tail approach.

### Data availability

The data that support the findings of our study are available from the corresponding author upon reasonable request.

## Results

### SI-CLP expression in TS/A adenocarcinoma cells inhibits tumor growth *in vivo*

To study the involvement of SI-CLP in the regulation of tumor growth, we have utilized subcutaneous mouse model of TS/A mammary adenocarcinoma in Balb/c female mice. Murine TS/A tumor cells and TS/A tumor tissues were found to be negative for endogenous SI-CLP expression. Similarly, human breast cancer tissues were either negative for SI-CLP expression (15/28 patients for German cohort vs. 26/52 patients for Russian cohort) or contained single SI-CLP positive cells in the tumor stroma, but not inside tumor cell islands (13/28 patients for German cohort vs. 26/52 patients for Russian cohort; Supporting Information Fig. S1). We did not find significant associations between clinical parameters of the patients and SI-CLP positive/negative status, which probably reflected scarce expression of SI-CLP in breast cancer tissue (Supporting Information Table S3). Thus, murine TS/A model of mammary adenocarcinoma was a suitable system to study the effect of SI-CLP delivery in the tumor mass using gain-of-function approach. TS/A cells were transfected either with empty vector (EV) or SI-CLP expression plasmid containing full-length murine SI-CLP fused to FLAG-tag (pcDNA3.1-SI-CLP-FLAG). Recombinant FLAG-tagged SI-CLP was efficiently expressed in TS/A cells transfected with SI-CLP expression plasmid, while no endogenous SI-CLP was detected in EV transfected TS/A cells (Fig. 1a). SI-CLP expression was also detectable in TS/A-SI-CLP tumor mass, but not in parental TS/A tumors or TS/A-EV tumors on day 21 after s.c. injection (Fig. 1b). Importantly, TS/A-SI-CLP tumor cells were able to secrete SI-CLP in the extracellular space (Fig. 1c). To study whether the presence of SI-CLP protein in TS/A tumor tissue influences tumor growth, TS/A-EV and TSA-SI-CLP cells were injected in Balb/c female mice and subcutaneous tumor growth was monitored for 21 day. The growth of SI-CLP expressing tumors was reduced 1.9 times on Day 7 ( $p < 0.0001$ ), 2.3 times on Day 10 ( $p < 0.0001$ ), 1.96 times on Day 14 ( $p < 0.0001$ ), 1.62 times on Day 18 ( $p = 0.0008$ ) and 1.61 times on Day 21 postinjection ( $p = 0.0153$ ; Figs. 1d–1h). Tumor weight was significantly lower in TS/A-SI-CLP group on Day 21 postinjection ( $p = 0.0363$ ; Fig. 1i). In order to assess whether SI-CLP suppressed tumor growth by direct effect on tumor cells, proliferation rates and migration capacities of TS/A-EV and TS/A-SI-CLP cells were compared, and no statistical differences were identified (Supporting Information Fig. S2). Thus, these intrinsic properties of TS/A cells were not affected by SI-CLP overexpression and did not contribute to the delayed

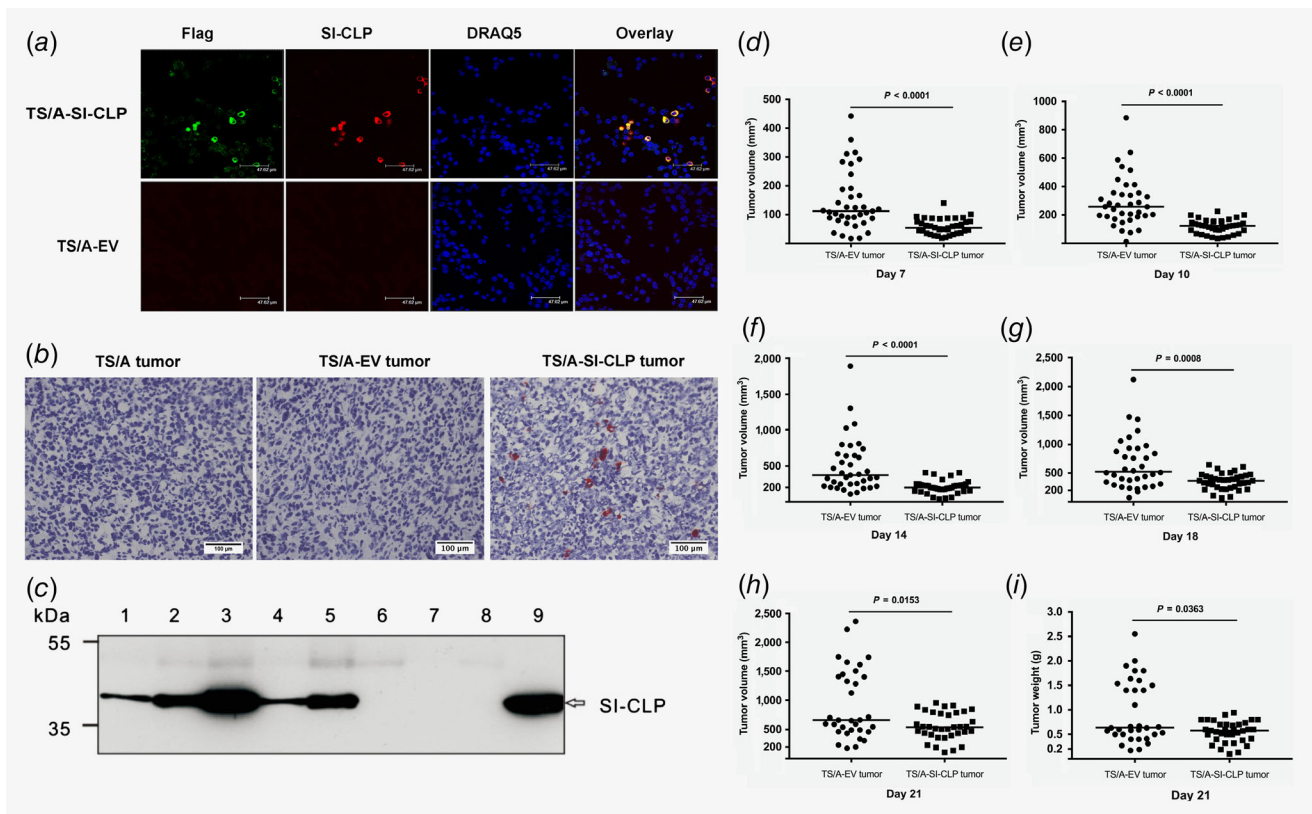


**Figure 1.** The dynamics of TS/A-EV and TS/A-SI-CLP tumor growth in Balb/c mice. (a) Immunofluorescent analysis of empty vector transfected (EV) and SI-CLP-FLAG transfected TS/A clones used for the injection in animal tumor model. FLAG tag was detected with rabbit anti-FLAG and Cy2-conjugated antirabbit secondary antibody (shown in green). SI-CLP was detected with rat-anti-SI-CLP antibody (clone 1B8) and Cy3-conjugated goat antirat secondary antibody (shown in red). Nuclei were visualized by DRAQ5 staining, scale bar: 47.62  $\mu\text{m}$ . (b) Immunohistochemical analysis of SI-CLP expression in TS/A-SI-CLP and TS/A-EV tumor tissues at Day 21 postinjection in Balb/c female mice using anti-SI-CLP rat mAb (1B8), scale bar: 100  $\mu\text{m}$ . (c) SI-CLP was precipitated from conditioned medium of TS/A-SI-CLP-FLAG cells using rabbit anti-FLAG antibody. Immunoprecipitated SI-CLP-FLAG was detected by Western blotting using anti-SI-CLP antibody (1B8). Lanes 1–5: TS/A-SI-CLP clones; Lanes 6–8: TS/A-vector clones, Lane 9: positive control (TS/A-SI-CLP cell lysate). (d–h) TS/A-EV and TS/A-SI-CLP cells were injected s.c. in Balb/c female mice and tumor volume was analyzed on Day 7 (d), Day 10 (e), Day 14 (f), Day 18 (g) and Day 21 (h) postinjection. Tumor weight (i) was measured at day 21 postinjection. Medians are indicated; Mann–Whitney U test was used for statistical analysis. The data are combined from five individual experiments using three TS/A-EV and three TS/A-SI-CLP clones. [Color figure can be viewed at [wileyonlinelibrary.com](http://wileyonlinelibrary.com)]

tumor growth *in vivo*. Therefore, next question was whether SI-CLP has an effect on the TME.

### Cellular composition of TME is altered in SI-CLP expressing tumors

We have examined whether reduced tumor size in TS/A-SI-CLP group is associated with the changes in the composition of TME by assessing vascularization and immune cell infiltration. TS/A-EV and TS/A-SI-CLP tumors were excised on Day 21 post-injection and analyzed using quantitative immunohistochemistry for the expression of cell-lineage and cell-activation markers including CD31 (vascular endothelium), CD68 (macrophages), CD206 and stabilin-1 (alternatively activated macrophages), Ly6G (neutrophils), Siglec-F (eosinophils), CD8 (cytotoxic T cells), CD4 (helper T cells) and FoxP3 (regulatory T cells). In contrast to the multiple reports indicating proangiogenic role of structurally related CLP protein YKL-40 in tumors, the

expression of SI-CLP in TS/A tumor tissue did not influence vascular density as assessed by CD31 expression (Fig. 2 and Supporting Information Fig. S3). In addition, the expression of neutrophil marker Ly6G and eosinophil marker Siglec-F was unchanged in EV and SI-CLP expressing tumors (Fig. 2 and Supporting Information Fig. S3). However, the expression of pan-macrophage marker CD68 as well as M2-associated markers CD206 and stabilin-1 was markedly decreased in SI-CLP expressing tumors suggesting inhibition of macrophage infiltration in the tumor tissue and/or changes in macrophages polarization status (Fig. 2 and Supporting Information Fig. S4). In parallel, the decrease was observed in the expression of T cell markers. Although tendency for the reduced amount of CD8+ cells in SI-CLP expressing tumors did not reach significance ( $p = 0.0907$ ), the reduction in CD4+ cells was statistically significant ( $p = 0.0185$ ) (Fig. 2 and Supporting Information Fig. S5). Of note, in TS/A-SI-CLP tumors, significant reduction was also

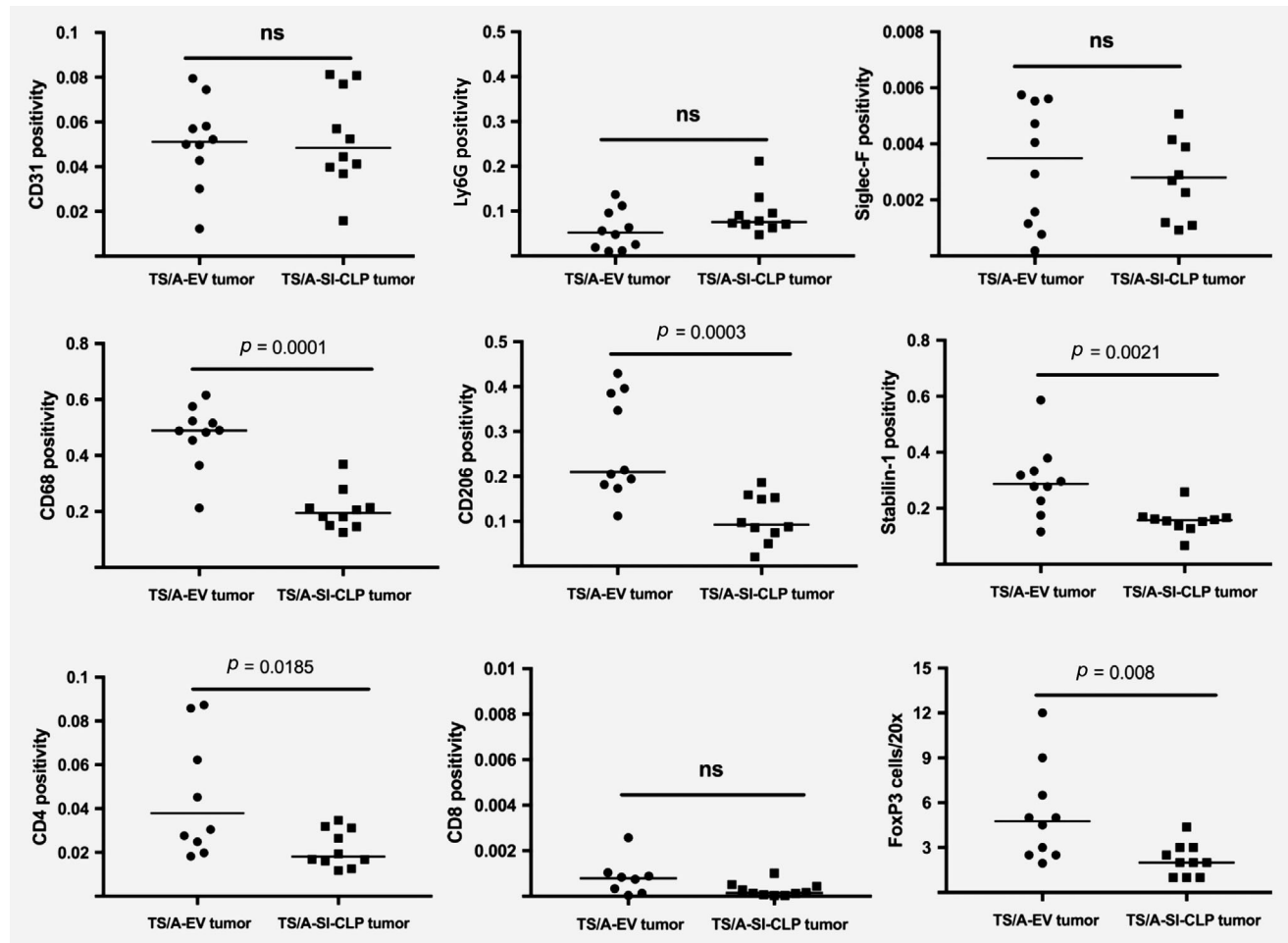


**Figure 2.** Cellular composition of the TME in TS/A-EV and TS/A-SI-CLP tumors. Tumors were injected s.c. and excised on Day 21 postinjection. Frozen sections were stained using immunohistochemistry for CD31 (vascular endothelium), Ly6G (neutrophils), Siglec-F (eosinophils), CD68 (pan-macrophage marker), CD206, stabilin-1 (markers of M2 macrophage polarization), CD8, CD4 (T cell markers) and FoxP3 (regulatory T cells). Entire sections were scanned and quantitatively analyzed using Aperio ImageScope software. Medians are indicated; Mann–Whitney U test was used for statistical analysis. ns, not significant.

observed in the expression of FoxP3 ( $p = 0.008$ ; Fig. 2 and Supporting Information Fig. S5) that is known to mark population of regulatory T cells involved in the suppression of antitumor immune response.

#### Macrophage activation is not affected in SI-CLP expressing tumors

Reduced expression of M2-associated markers CD206 and stabilin-1 in SI-CLP expressing tumor tissues suggested that tumor-inhibiting effect of SI-CLP can be at least partially mediated by macrophage repolarization toward proinflammatory antitumor phenotype. To examine this, TAM were isolated from TS/A-EV and TS/A-SI-CLP tumors on Day 21 postinjection and subjected to RT-qPCR analysis of arginase I, macrophage scavenger receptors (CD163, stabilin-1, CD206), proinflammatory cytokines TNF- $\alpha$ , IL-1 $\beta$  and IL-6, and tumor supporting cytokines/growth factors IL-10, TGF $\beta$  and VEGF-A. No statistically significant difference in the expression of all analyzed genes was

detected between EV and SI-CLP expressing tumors (Fig. 3). A tendency for the increased expression of CD163 and cytokines was observed in TAM isolated from SI-CLP expressing tumors. However, this effect did not reach statistical significance. This data indicated that reduced positivity for CD206 and stabilin-1 in SI-CLP expressing tumors is primarily caused by impaired accumulation of M2-like polarized TAM in the tumor tissue rather than changes in TAM phenotype.

#### SI-CLP impairs CCL2-induced monocyte and macrophage migration

To clarify the mechanism of reduced TAM infiltration in SI-CLP expressing tumors, we have tested whether SI-CLP directly influences monocyte and macrophage migration *in vitro* in the transwell system. Effect of SI-CLP was assessed by two approaches: direct application in the bottom chamber or pre-incubation with BMDM. Migration was induced by addition in the lower chamber of 100 ng/ml of murine CCL2, major

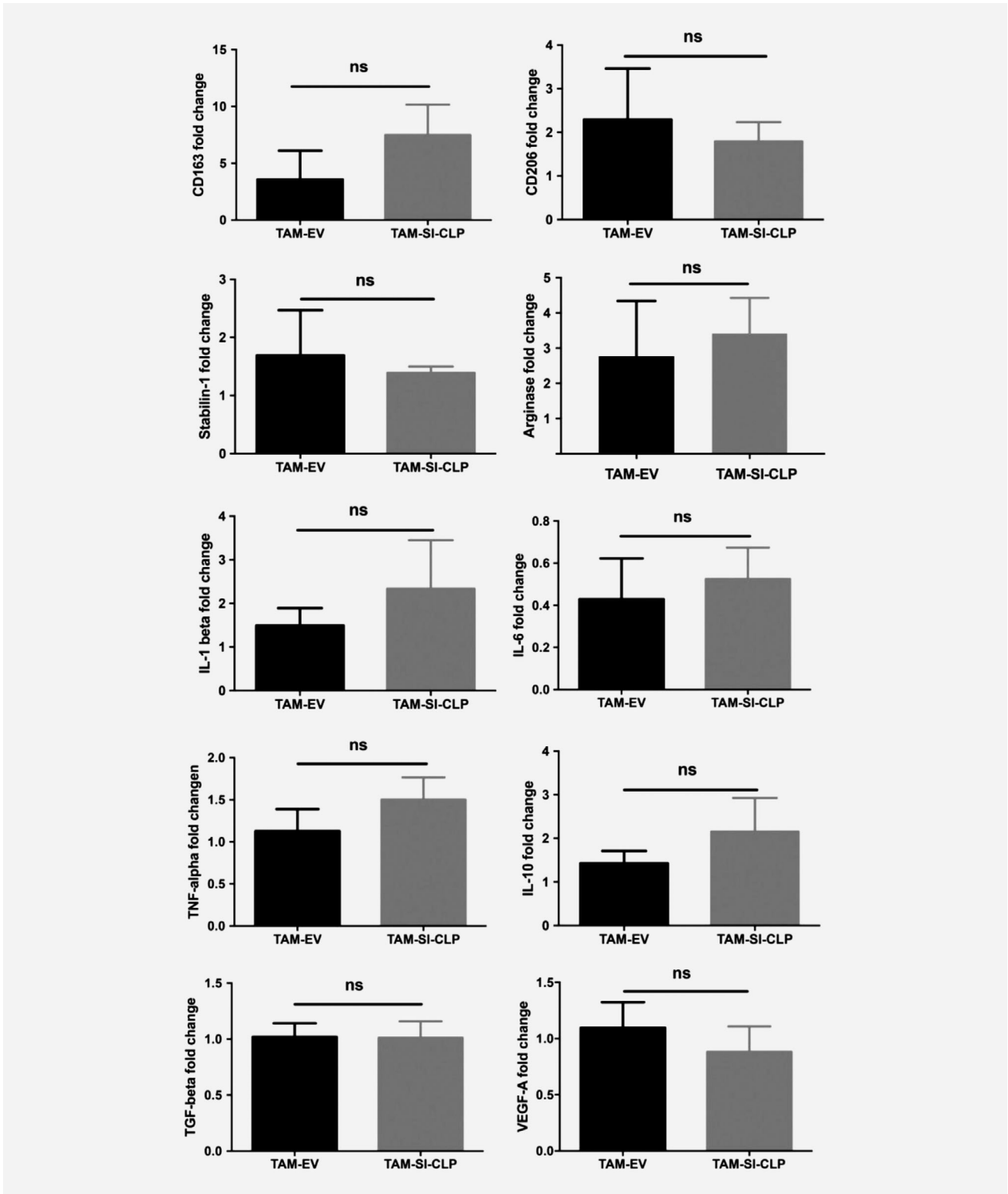


**Figure 3.** The comparison of TAM phenotype in TS/A-EV and TS/A-SI-CLP tumors. TAM were isolated from TS/A-EV and TS/A-SI-CLP tumors and subjected to the analysis of the expression of CD163, CD206, stabilin-1, TNF- $\alpha$ , IL-6, IL-1 $\beta$ , IL-10, TGF $\beta$ , arginase I and VEGFA using RT-qPCR. Four clones of TS/A-EV and TS/A-SI-CLP cells were used for injection. For each clone, TAM were pooled from five mice. The data are presented as mean  $\pm$  SD; unpaired *t*-test was used for statistical analysis; ns, not significant.



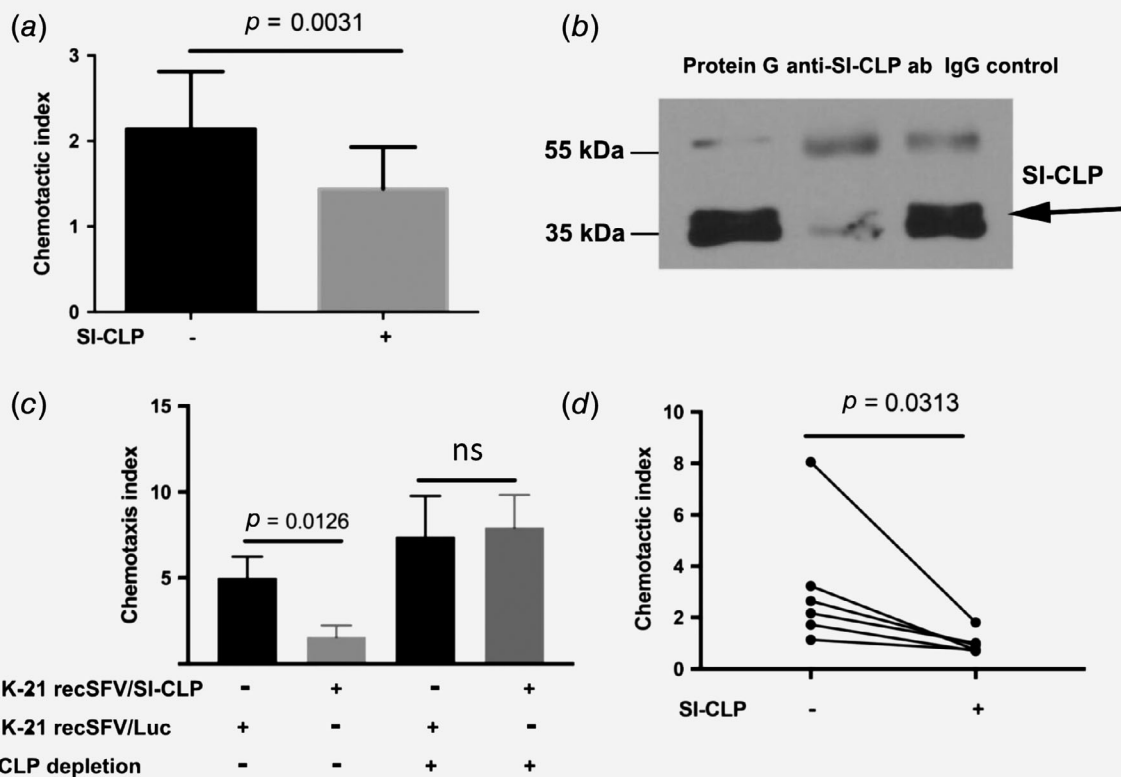


**Figure 4.** The effect of SI-CLP on the migration of monocytes and macrophages. (a) BMDM were generated in Balb/c mice ( $n = 5$ ) and incubated for 30 min with 100 ng/ml of purified murine SI-CLP. BMDM ( $5 \times 10^5$ ) were allowed to migrate toward 100 ng/ml of murine CCL2 in RPMI medium for 3 hr. The chemotactic index was calculated by dividing the number of migrated cells in SI-CLP group by the number of migrated cells in control group (without SI-CLP). The experiment was performed in triplicates and data are presented as mean  $\pm$  SD; unpaired *t*-test was used for statistical analysis. (b) SI-CLP containing supernatants obtained from BHK-21 producer cells infected with SI-CLP-encoding recSFV were subjected to SI-CLP depletion using rat anti SI-CLP antibodies (clone 1B8) bound to protein G beads. Empty protein G beads or beads bound to rat IgG were used as a control. Depleted supernatants were analyzed by Western blotting using anti SI-CLP (1B8) antibodies. (c) BMDM were preincubated for 16 hr either with intact supernatants or SI-CLP depleted supernatants derived from BHK-21 cells infected with recSFVEnh/SI-CLP or recSFVEnh/Luc (control) followed by migration for 3 hr toward 100 ng/ml CCL2. Data are presented as mean  $\pm$  SD; unpaired *t*-test was used for statistical analysis; ns, not significant. (d) Monocytes were isolated from six healthy donors and preincubated with purified human SI-CLP for 16 hr in macrophage SFM medium. Monocytes ( $1 \times 10^5$ ) were allowed to migrate toward 100 ng/ml of human CCL2 for 3 hr. Migrated cells were analyzed on the lower side of the membrane. Paired *t*-test was used for the data analysis.

chemotactic factor for monocytes and macrophages in the TME. Addition of SI-CLP in the bottom chamber did not change migration of BMDM toward CCL2 ( $p = 0.177$ , Supporting Information Fig. S6). However, preincubation of BMDM with SI-CLP prior to the migration assays had a statistically significant inhibitory effect (1.55 times,  $p = 0.0031$ ) on their recruitment by CCL2 (Fig. 4a). This inhibitory effect was confirmed by another source of SI-CLP, the conditioned supernatant of BHK-21 cells infected with SI-CLP encoding alphavirus (recSFVEnh/SI-CLP) and controlled by the supernatant of recSFVEnh/Luc control virus infected cells. Statistically significant inhibitory effect of virus-derived SI-CLP on the migration of BMDM was identified (3.2 times,  $p = 0.0126$ ; Fig. 4c). Furthermore, to demonstrate specific effect of SI-CLP on BMDM migration, SI-CLP protein was depleted from recSFVEnh/SI-CLP supernatants by immunoprecipitation using rat anti-SI-CLP

antibody immobilized on protein G beads (Fig. 4b). Incubation of BMDM with SI-CLP depleted supernatants resulted in complete restoration of migration capacity of BMDM (Fig. 4c).

We have also assessed the effect of purified human SI-CLP on the migration of human CD14<sup>+</sup> monocytes derived from six healthy donors. SI-CLP significantly inhibited human monocyte migration toward CCL2 (Fig. 4d). Moreover, SI-CLP also inhibited monocyte migration in response to another CCR2 ligand CCL7, which is expressed in breast cancer.<sup>20</sup> However, this effect did not reach statistical significance (Supporting Information Fig. S7). Similarly, the effect of SI-CLP on monocyte migration toward CCR1/CCR3/CCR5-interacting chemokine CCL5 was not statistically significant, although decreased migration was observed in four out of six analyzed donors (Supporting Information Fig. S7).

Since SI-CLP significantly impaired monocyte migration toward CCR2 ligand CCL2, we next assessed whether SI-CLP influenced CCR2 expression in human and mouse monocytes/macrophages. CCR2 gene expression levels were modestly decreased in mouse TAM isolated from SI-CLP expressing tumors, although the difference did not reach statistical significance (Supporting Information Fig. S8A). In human monocytes incubated with 100 ng/ml SI-CLP for 16 hr, the expression of CCR2 was not changed both at the mRNA and protein level (Supporting Information Figs. S8B and S8C).

Furthermore, we have hypothesized that the ability of SI-CLP to bind multiple sugar moieties could enable SI-CLP interaction with glycosylated regions in extracellular loops of CCR2,<sup>21,22</sup> resulting in blockade of CCR2 ligand-binding sites. To test whether SI-CLP prevents CCR2/CCL2 interaction, we examined CCR2 internalization—an event that quickly follows the binding of CCL2 to CCR2.<sup>23,24</sup> Preincubation of monocytes with SI-CLP for 16 hr did not significantly alter surface expression of CCR2 (Supporting Information Fig. S9A and S9B). Furthermore, SI-CLP neither affected CCL2-induced CCR2 internalization nor subsequent CCR2 recycling on the cell surface (Supporting Information Fig. S9C), indicating that CCL2/CCR2 interaction and

monocyte responsiveness to CCL2 were not compromised in the presence of SI-CLP.

To address whether inhibited migration of monocytes in the presence of SI-CLP was associated with changes in cytoskeleton, we incubated monocytes in the presence of SI-CLP for 16 hr followed by 30 min stimulation with CCL2 and assessment of actin and tubulin distribution using fluorescent microscopy. Stimulation of monocytes with CCL2 in the absence of SI-CLP induced the recruitment of tubulin into actin-rich lamellipodia-like protrusions (Fig. 5, indicated by arrows). In the presence of SI-CLP, CCL2-induced protrusions were less abundant and characterized by decreased recruitment of tubulin (Fig. 5). Overall, SI-CLP-mediated inhibition of monocyte migration was associated with suppression of CCL2-induced cytoskeletal rearrangements.

#### SI-CLP has no direct effect on the migration of T-cells

Reduced numbers of CD4+ and CD8+ positive cells in SI-CLP expressing TS/A tumors prompted us to examine whether SI-CLP can directly influence T cells migration toward chemotactic stimuli. Splenic T cells were isolated from WT Balb/c mice and preincubated with purified murine SI-CLP for 16 hr

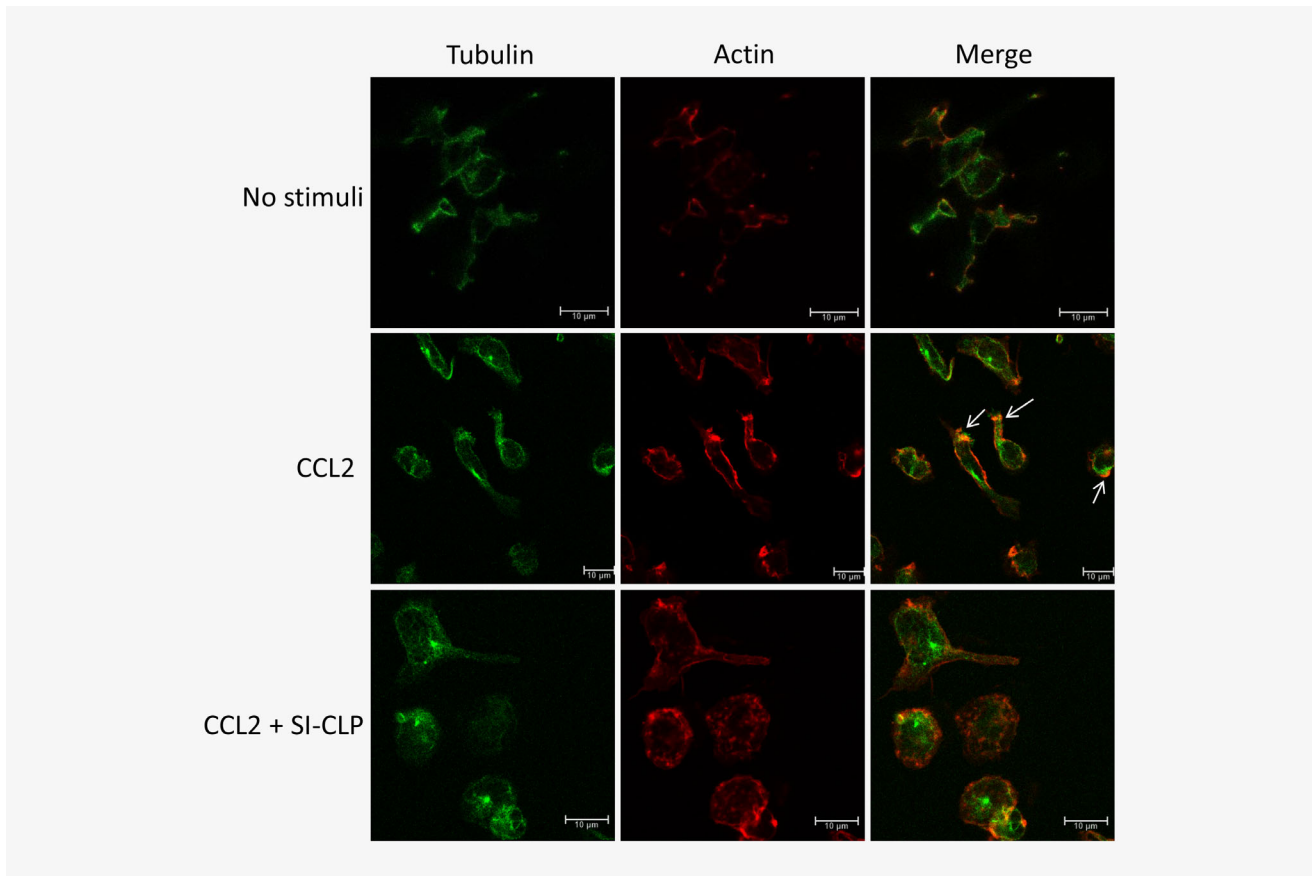


**Figure 5.** The effect of SI-CLP on cytoskeleton. Primary monocytes isolated from healthy donors were incubated with SI-CLP for 16 hr followed by stimulation with CCL2 for 30 min. Cells were fixed, stained using phalloidin and antitubulin antibodies and examined by fluorescent/confocal microscopy. Representative images are shown. Scale bars: 10 µm. [Color figure can be viewed at [wileyonlinelibrary.com](http://wileyonlinelibrary.com)]

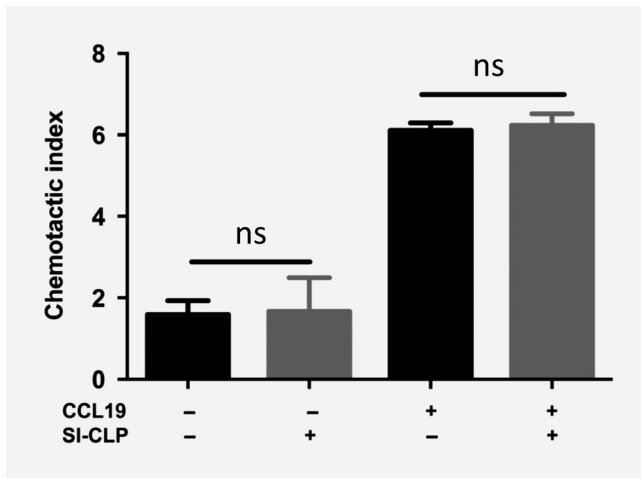


**Figure 6.** The effect of SI-CLP on the migration of murine T cells. Naïve T cells were isolated from spleens of Balb/c mice and incubated with murine SI-CLP for 16 hr followed by migration toward murine CCL19 for 3 hr. Migrated cells were counted in the lower chamber. The data are combined for three experiments (three mice in each) and presented as mean  $\pm$  SD; unpaired *t*-test was used for statistical analysis; ns, not significant.

followed by assessment of T cell migration in steady state conditions or toward 100 ng/ml of CCL19 (Fig. 6). In contrast to murine macrophages, SI-CLP did not affect T cell migration in the absence or presence of chemotactic stimuli (Fig. 6). These data indicated that decreased amount of T-cells in the TME is indirect effect of SI-CLP expression in the tumor.

## Discussion

In the current study, we identify for the first time antitumor effect of SI-CLP related to the suppression of TAM recruitment in a mouse model of breast cancer. Subcutaneous growth of TS/A tumors expressing SI-CLP was significantly delayed compared to EV-transfected tumors despite similar proliferation and migration rates in TS/A-SI-CLP and TS/A-EV tumor cells. Since intrinsic properties of tumor cells were not altered by SI-CLP expression, changes in the composition of TME in SI-CLP expressing tumors were likely to cause inhibition of tumor growth. Indeed, IHC analysis revealed significant decrease in TAM infiltration into SI-CLP expressing tumors. In breast cancer, multiple studies indicated the association of TAM infiltration with poor prognosis and their direct involvement in the support of tumor growth and tumor cell invasion.<sup>25–27</sup> Moreover, the accumulation of CD206+ and stabilin-1+ TAM subsets was associated with tumor growth promotion in animal breast cancer models and/or breast cancer patients.<sup>14,28,29</sup> In our study, the expression of protumor macrophage markers CD206 and stabilin-1 was significantly lower in SI-CLP expressing tumors suggesting reduced accumulation of tumor-supportive TAM subsets in the tumor tissue. Therefore, based on multiple reports, reduction in TAM density was interpreted as the main factor underlying antitumor effect of SI-CLP. Additional *in vitro* studies showed that SI-CLP protein strongly

impaired migration of human monocytes and mouse macrophages toward major macrophage chemoattractant CCL2. The expression of CCL2 was previously shown to be elevated in TAM and tumor cells in breast cancer and other types of cancer, and resulted in enhanced monocyte recruitment in the tumor site.<sup>30–32</sup> Disrupting CCL2/CCR2 axis in cancer using CCL2 neutralizing antibodies reduced tumor growth and potentiated the effects of tumor vaccines and chemotherapy.<sup>33,34</sup> Moreover, SI-CLP inhibited the migration of monocytes toward other chemokines expressed in breast cancer tissue, CCL7 and CCL5,<sup>20</sup> although these effects were donor-dependent and did not reach statistical significance. Thus, SI-CLP may have potential advantages in inhibition of TAM recruitment to the tumor mass compared to CCL2 neutralizing antibodies due to its ability to inhibit monocyte migration toward multiple chemokines produced in breast cancer tissue.

The results of the present study suggested that the inhibition of CCL2-induced monocyte migration by SI-CLP was not due to the suppression of CCR2/CCL2 interaction or activation of downstream effectors. In addition, we have observed SI-CLP-mediated inhibition of monocyte migration in response to CCR2 ligands CCL2 and CCL7 as well as CCR1/CCR3/CCR5 ligand CCL5. Therefore, low specificity of observed effects suggests that SI-CLP may interfere with other common components of cell migration machinery resulting in suppression of ligand-induced cytoskeletal rearrangements. Indeed, another member of CLP family YKL-40 was found to influence motility of endothelial cells through activation of integrin signaling and regulated glioma cell migration *via* modulation of cell adhesion to certain ECM components.<sup>35,36</sup> The interaction of SI-CLP with these pathways needs to be addressed in the future studies.

Altogether, our data indicate that SI-CLP interferes with chemokine-induced accumulation of TAM in the TME. Therefore, the use of SI-CLP as an inhibitor of TAM recruitment can be considered for therapeutic application in the treatment of breast cancer.

Although expression of T cell markers CD4 and FoxP3 was significantly lower in SI-CLP expressing tumors, purified SI-CLP did not directly affect migration of splenic T cells in the steady state or in the presence of chemotactic factor CCL19. Since TAM were shown to produce wide range of chemotactic factors that recruit Tregs, naive T cells and Th2 cells into tumors,<sup>37,38</sup> decreased infiltration of T cell subsets in SI-CLP expressing tumors could be explained by reduced TAM infiltration in the tumor tissue that leads to deficiency in T cell recruiting factors.

Interestingly, the results of the present study suggest that SI-CLP have opposite function in the regulation of tumor growth when compared to YKL-40 and YKL-39 proteins. Although all of these proteins belong to Glyco\_18 domain-containing protein family and share certain structural organization, SI-CLP has the lowest degree of similarity with other CLP proteins and contains unique sequence between signal peptide and Glyco\_18 domain.<sup>12</sup> Functionally, overexpression of YKL-40 in breast cancer and colorectal cancer cell lines was shown to stimulate proliferation of

cancer cells *in vitro* and aggravate subcutaneous tumor growth *in vivo*.<sup>10,39</sup> YKL-40 expression facilitated angiogenesis in transplant mouse models of colorectal cancer and glioblastoma.<sup>40</sup> In addition, YKL-40 expression in HCT116 xenografted colorectal tumors was associated with increased macrophage accumulation in the tumor tissue.<sup>10</sup> Similarly, YKL-39 protein stimulated angiogenesis and monocyte migration, and was associated with increased risk of distant metastasis after NAC in breast cancer patients.<sup>11</sup> In our current study, overexpression of SI-CLP protein in breast cancer TS/A cell line did not significantly affect tumor cell proliferation, but resulted in markedly impaired tumor growth *in vivo*. Microvessel density was not affected by SI-CLP expression in the tumor tissue. However, strong reduction in macrophage migration and TAM accumulation in the tumor was observed. Differential effects of YKL-40, YKL-39 and SI-CLP on cell migration are presumably mediated by the way of interaction of these proteins with cell surface. Several cell surface receptors were identified for YKL-40 including syndecan-1 on endothelial and glioblastoma cells, receptor for advanced glycosylation end products on mouse intestinal epithelial cells and IL13R2 on macrophages and airway epithelial cells.<sup>41–43</sup> The interaction of YKL-40 with these receptors resulted in stimulation of endothelial cell tube formation, proliferative and antiapoptotic effects in epithelial cells, VEGF production by tumor cells and increased

angiogenesis.<sup>9</sup> Despite certain structural similarity between SI-CLP and YKL-40, the potential interaction of SI-CLP with above-mentioned receptors was not characterized and remains to be identified.

Overall, the results of our study propose SI-CLP as a novel soluble tumor growth suppressing factor that mediates its antitumor effects through prevention of chemokine-induced TAM infiltration in the tumor tissue. The results of our study warrant further investigation of SI-CLP protein as a novel molecular agent that interferes with TAM recruitment in the tumor tissue, which is of clinical relevance in human breast cancer.

### Acknowledgements

The study was supported by ERA.NET RUS DTEST-CLP and ERA.Net RUS Plus CHIT-ALPHA-THER grants. The analysis of SI-CLP expression in breast cancer patient cohort at Tomsk Cancer Research Institute (illustrated by Supporting Information Fig. S1) as well as analysis of associations between SI-CLP expression and clinical parameters (illustrated by Supporting Information Table S3) was supported by Russian Science Foundation, grant #14-15-00350. The PhD positions of Shuiping Yin and Nan Wang were supported by the program of China Scholarships Council (No. 201208080046 and 2009616122, respectively). The authors gratefully acknowledge the technical assistance of Ms. Maria Deligianni (Institute of Pathology, Medical Faculty Mannheim), and the support of Stefanie Uhlh, operating the Mannheimer FlowCore Facility.

### References

- Quail DF, Joyce JA. Microenvironmental regulation of tumor progression and metastasis. *Nat Med* 2013;19:1423–37.
- Biswas SK. Metabolic reprogramming of immune cells in cancer progression. *Immunity* 2015;43:435–49.
- Rabinovich GA, Gabrilovich D, Sotomayor EM. Immunosuppressive strategies that are mediated by tumor cells. *Annu Rev Immunol* 2007;25:267–96.
- Szebeni GJ, Vizler C, Kitajka K, et al. Inflammation and cancer: extra- and intracellular determinants of tumor-associated macrophages as tumor promoters. *Mediators Inflamm* 2017;2017:9294018.
- Mantovani A, Allavena P. The interaction of anti-cancer therapies with tumor-associated macrophages. *J Exp Med* 2015;212:435–45.
- Pienta KJ, Machiels JP, Schrijvers D, et al. Phase 2 study of carlumab (CNTO 888), a human monoclonal antibody against CC-chemokine ligand 2 (CCL2), in metastatic castration-resistant prostate cancer. *Invest New Drugs* 2013;31:760–8.
- Sandhu SK, Papadopoulos K, Fong PC, et al. A first-in-human, first-in-class, phase I study of carlumab (CNTO 888), a human monoclonal antibody against CC-chemokine ligand 2 in patients with solid tumors. *Cancer Chemother Pharmacol* 2013;71:1041–50.
- Bonapace L, Coissieux MM, Wyckoff J, et al. Cessation of CCL2 inhibition accelerates breast cancer metastasis by promoting angiogenesis. *Nature* 2014;515:130–3.
- Kzhyshkowska J, Yin S, Liu T, et al. Role of chitinase-like proteins in cancer. *Biol Chem* 2016;397:231–47.
- Kawada M, Seno H, Kanda K, et al. Chitinase 3-like 1 promotes macrophage recruitment and angiogenesis in colorectal cancer. *Oncogene* 2012;31:3111–23.
- Liu T, Larionova I, Litviakov N, et al. Tumor-associated macrophages in human breast cancer produce new monocyte attracting and pro-angiogenic factor YKL-39 indicative for increased metastasis after neoadjuvant chemotherapy. *Oncimmunology* 2018;7:e1436922.
- Kzhyshkowska J, Mamidi S, Gratchev A, et al. Novel stabilin-1 interacting chitinase-like protein (SI-CLP) is up-regulated in alternatively activated macrophages and secreted via lysosomal pathway. *Blood* 2006;107:3221–8.
- Xiao W, Meng G, Zhao Y, et al. Human secreted stabilin-1-interacting chitinase-like protein aggravates the inflammation associated with rheumatoid arthritis and is a potential macrophage inflammatory regulator in rodents. *Arthritis Rheumatol* 2014;66:1141–52.
- Riabov V, Yin S, Song B, et al. Stabilin-1 is expressed in human breast cancer and supports tumor growth in mammary adenocarcinoma mouse model. *Oncotarget* 2016;7:31097–110.
- Gratchev A, Kzhyshkowska J, Utikal J, et al. Interleukin-4 and dexamethasone counterregulate extracellular matrix remodelling and phagocytosis in type-2 macrophages. *Scand J Immunol* 2005;61:10–7.
- Vasilevska J, Skrastina D, Spunde K, et al. Semliki Forest virus biodistribution in tumor-free and 4T1 mammary tumor-bearing mice: a comparison of transgene delivery by recombinant virus particles and naked RNA replicon. *Cancer Gene Ther* 2012;19:579–87.
- Kurena B, Müller E, Christopoulos PF, et al. Generation and functional in vitro analysis of semliki Forest virus vectors encoding TNF- $\alpha$  and iFN- $\gamma$ . *Front Immunol* 2017;8:1667.
- Zajakina A, Vasilevska J, Zhulenkovs D, et al. High efficiency of alphaviral gene transfer in combination with 5-fluorouracil in a mouse mammary tumor model. *BMC Cancer* 2014;14:460.
- van Gils JM, Derby MC, Fernandes LR, et al. The neuroimmune guidance cue netrin-1 promotes atherosclerosis by inhibiting the emigration of macrophages from plaques. *Nat Immunol* 2012;13:136–43.
- Thomas JK, Mir H, Kapur N, et al. CC chemokines are differentially expressed in breast cancer and are associated with disparity in overall survival. *Sci Rep* 2019;9:4014.
- Meng G, Zhao Y, Bai X, et al. Structure of human stabilin-1 interacting chitinase-like protein (SI-CLP) reveals a saccharide-binding cleft with lower sugar-binding selectivity. *J Biol Chem* 2010;285:39898–904.
- Preobrazhensky AA, Dragan S, Kawano T, et al. Monocyte chemotactic protein-1 receptor CCR2B is a glycoprotein that has tyrosine sulfation in a conserved extracellular N-terminal region. *J Immunol* 2000;165:5295–303.
- Carvalho L, Lopez L, Che F-Y, et al. Buprenorphine decreases the CCL2-mediated chemotactic response of monocytes. *J Immunol* 2015;194:3246–58.
- Lopez MG, Martínez AA, Lamaze C, et al. Inhibition of dynamin prevents CCL2-mediated endocytosis of CCR2 and activation of ERK1/2. *Cell Signal* 2009;21:1748–57.

25. Noy R, Pollard JW. Tumor-associated macrophages: from mechanisms to therapy. *Immunity* 2014;41:49–61.
26. Qian BZ, Pollard JW. Macrophage diversity enhances tumor progression and metastasis. *Cell* 2010;141:39–51.
27. Zhang QW, Liu L, Gong CY, et al. Prognostic significance of tumor-associated macrophages in solid tumor: a meta-analysis of the literature. *PLoS One* 2012;7:e50946.
28. Chen EP, Markosyan N, Connolly E, et al. Myeloid cell COX-2 deletion reduces mammary tumor growth through enhanced cytotoxic T-lymphocyte function. *Carcinogenesis* 2014;35:1788–97.
29. Luo Y, Zhou H, Krueger J, et al. Targeting tumor-associated macrophages as a novel strategy against breast cancer. *J Clin Invest* 2006;116:2132–41.
30. Ben-Baruch A. Host microenvironment in breast cancer development: inflammatory cells, cytokines and chemokines in breast cancer progression: reciprocal tumor-microenvironment interactions. *Breast Cancer Res* 2003;5:31–6.
31. Erreni M, Mantovani A, Allavena P. Tumor-associated macrophages (TAM) and inflammation in colorectal cancer. *Cancer Microenviron* 2011;4:141–54.
32. Raman D, Baugher PJ, Thu YM, et al. Role of chemokines in tumor growth. *Cancer Lett* 2007;256:137–65.
33. Fridlender ZG, Buchlis G, Kapoor V, et al. CCL2 blockade augments cancer immunotherapy. *Cancer Res* 2010;70:109–18.
34. Moisan F, Francisco EB, Brozovic A, et al. Enhancement of paclitaxel and carboplatin therapies by CCL2 blockade in ovarian cancers. *Mol Oncol* 2014;8:1231–9.
35. Ku BM, Lee YK, Ryu J, et al. CHI3L1 (YKL-40) is expressed in human gliomas and regulates the invasion, growth and survival of glioma cells. *Int J Cancer* 2011;128:1316–26.
36. Shao R, Hamel K, Petersen L, et al. YKL-40, a secreted glycoprotein, promotes tumor angiogenesis. *Oncogene* 2009;28:4456–68.
37. Hao NB, Lu MH, Fan YH, et al. Macrophages in tumor microenvironments and the progression of tumors. *Clin Dev Immunol* 2012;2012:948098.
38. Liu J, Zhang N, Li Q, et al. Tumor-associated macrophages recruit CCR6+ regulatory T cells and promote the development of colorectal cancer via enhancing CCL20 production in mice. *PLoS One* 2011;6:e19495.
39. Libreros S, Garcia-Areas R, Iragavarapu-Charyulu V. CHI3L1 plays a role in cancer through enhanced production of pro-inflammatory/pro-tumorigenic and angiogenic factors. *Immunol Res* 2013;57:99–105.
40. Faibish M, Francescone R, Bentley B, et al. A YKL-40-neutralizing antibody blocks tumor angiogenesis and progression: a potential therapeutic agent in cancers. *Mol Cancer Ther* 2011;10:742–51.
41. Francescone RA, Scully S, Faibish M, et al. Role of YKL-40 in the angiogenesis, radioresistance, and progression of glioblastoma. *J Biol Chem* 2011;286:15332–43.
42. He CH, Lee CG, Cruz CSD, et al. Chitinase 3-like 1 regulates cellular and tissue responses via IL-13 receptor  $\alpha 2$ . *Cell Rep* 2013;4:830–41.
43. Low D, Subramaniam R, Lin L, et al. Chitinase 3-like 1 induces survival and proliferation of intestinal epithelial cells during chronic inflammation and colitis-associated cancer by regulating S100A9. *Oncotarget* 2015;6:36535.